Structure and Dynamics of Phthalocyanine–Argon$_n$ ($n = 1-4$) Complexes Studied in Helium Nanodroplets[†]

Rudolf Lehnig,[‡] Joshua A. Sebree,[§] and Alkwin Slenczka*

Institut für Physikalische und Theoretische Chemie, Universität Regensburg, Regensburg, Germany

Received: January 31, 2007; In Final Form: March 29, 2007

Van der Waals clusters of phthalocyanine with 1−4 argon atoms formed inside superfluid helium nanodroplets have been investigated by recording fluorescence excitation spectra as well as emission spectra. The excitation spectra feature a multitude of sharp lines when recorded in superfluid helium droplets in contrast to the respective spectra measured in a seeded supersonic beam (Cho et al. *Chem. Phys. Lett.* **2000**, *326*, 65). The pickup technique used for doping of the phthalocyanine and the argon into the droplets allows for nondestructive analysis of the cluster sizes. Alternation of the pickup sequence gives information on the binding site of the argon atoms. The investigation of dispersed emission spectra in helium droplets can be used as a special tool for the identification of 0_0^0 transitions within the variety of sharp lines seen in the excitation spectra. Thus, different isomers of the clusters can be distinguished. Moreover, the emission spectra reveal information on dynamic processes such as vibrational predissociation of the van der Waals complexes and interconversion among isomeric species. The binding energy of the phthalocyanine–argon$_1$ complex in helium droplets was estimated to be at most 113 cm^{-1}.

1. Introduction

Molecular clusters consisting of a single organic molecule and several rare gas atoms can be viewed as model systems for studying the transition from a single isolated molecule to a molecule fully dissolved in a macroscopic solvent bath. Considerable interest is therefore directed toward the analysis of the energetics, the structure, and the dynamics of these clusters.[1−8] This paper presents excitation and emission spectroscopy of the van der Waals clusters composed of a single phthalocyanine molecule (Pc) and one up to four argon (Ar) atoms.

Recently, it has been shown that helium droplets serving as a cryogenic and very gentle matrix are particularly suited for the design and spectroscopic investigation of van der Waals clusters.[9−14] An important feature of spectroscopy in helium droplets is that quasi solvent-free spectra are observed. Also, clusters of a well-defined size can be easily formed within helium droplets by doping the droplets consecutively with single atoms or molecules that coagulate inside the droplets. The kinetic and internal energy of each molecule or atom as well as the binding energy released by complexation are dissipated into the helium droplet and finally released from the droplet by evaporative cooling within picoseconds.[15] Thereby, molecular aggregates inside helium droplets relax to a temperature of 0.38 K.[16,10] One advantage of the pickup technique is the control over the number of dopants within a helium droplet by changing the pressure of the dopant molecule in the pickup cell. Because the doping process obeys Poisson statistics, the number of doped particles and therefore the size of the cluster formed inside the droplet can be analyzed without destroying the cluster.[9] By alternating the doping sequence, structural details can be deduced for clusters consisting of different moieties.[12]

This paper demonstrates the advantages of dispersed emission spectra as a new experimental tool for cluster research in helium droplets. With the help of emission spectra, electronic origins can be identified among the large number of sharp transitions observed in the excitation spectra. Hence, different isomers for each cluster size can be distinguished. Moreover, dynamic effects such as dissociation and configurational relaxation can be observed.

The present paper is organized as follows: After a brief description of the experimental setup, the results obtained from the excitation and emission spectra of PcAr$_n$ ($n = 1-4$) in helium droplets will be presented. The clusters will be analyzed according to size and structure, and the results will be compared to the spectra obtained in a seeded supersonic jet.[7] Subsequently, dynamic effects revealed by the emission spectra will be discussed.

2. Experimental Setup

The setup of the helium droplet spectrometer follows the design outlined in ref 17 and has been described in detail in ref 18. Therefore, this section addresses only the aspects that are of interest for the current experiment.

All of the measurements were performed with helium droplets produced by expanding helium gas through a 5 μm nozzle at a stagnation pressure of 20 bar and at a nozzle temperature of 10.3 K, leading to an average droplet size of 20000 atoms.[19] The droplet beam was collimated by a 0.7 mm skimmer located 3 cm from the nozzle and entered a differentially pumped chamber. At a distance of about 10 cm from the nozzle, the droplets passed through an oven, which served as a sublimation scattering cell for doping with Pc. Two additional pickup cells were mounted before and behind the oven. They were connected to a gas inlet system fed by Ar gas for additional doping with Ar before or after the doping with Pc, respectively. The Ar pressure in the two pickup cells was tuned by two leak valves

Phthalocyanine−Argon_n Complexes

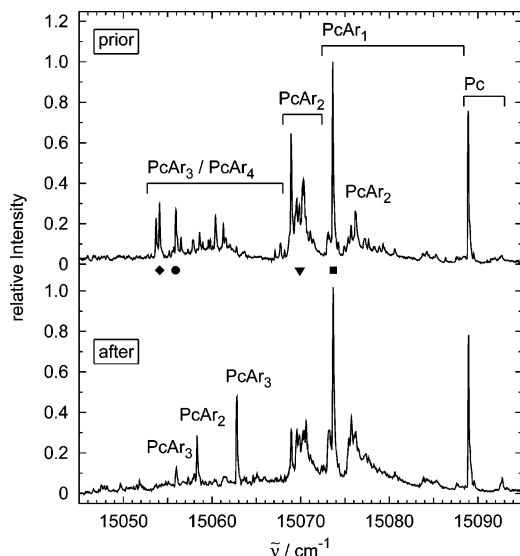*J. Phys. Chem. A, Vol. 111, No. 31, 2007* **7577**

Figure 1. Fluorescence excitation spectra of phthalocyanine (Pc) and various phthalocyanine−argon complexes (PcAr$_n$, $n = 1-4$) in helium droplets ($\bar{N} \approx 20000$) in the range from 15045 to 15095 cm^{-1}. The upper trace shows a spectrum that was obtained when Ar was doped into the droplets prior to Pc, and the lower trace represents the spectrum for a pickup of Ar after Pc. The Ar pressure for both spectra was optimized for a maximum signal of the PcAr$_2$ complex.
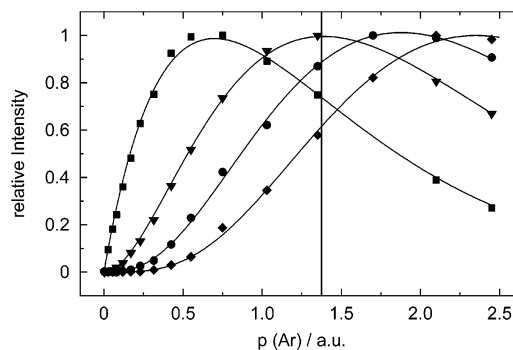

Figure 2. Intensity of four peaks of the excitation spectrum measured by doping Ar prior to Pc (upper trace in Figure 1) at 15073.7 (squares), 15069.0 (triangles), 15055.9 (circles), and 15054.1 cm^{-1} (diamonds) as a function of the Ar pressure in the doping cell. These four peaks are marked in Figure 1 with the same symbols. The solid lines represent fits with eq 1 for $n = 1$, 2, 3, or 4. The vertical line marks the Ar pressure that leads to a maximum signal of the PcAr$_2$ complex and that was chosen for the measurement of the spectra in Figure 1.

and monitored by the pressure increase in the entire vacuum chamber. For the current experiments, the oven temperature was optimized for single molecule doping of Pc. The doped droplet beam was crossed 40 mm behind the pickup unit perpendicularly by the beam of a continuously tunable single-mode ring dye laser (specified bandwidth of <1 MHz). The fluorescence light was collected perpendicular to both the droplet beam and the laser beam with a lens and focused with a second lens onto the first cathode of a photomultiplier or onto the entrance slit of a spectrograph (focal length of 50 cm) equipped with a CCD camera (256 pixels × 1024 pixels). At a wavenumber of 15000 cm^{-1}, every row of the CCD chip covered a wavenumber interval of 0.8 cm^{-1}. The experimentally determined spectral resolution of the spectrograph was about 1.8 cm^{-1}. A commercially available sample of phthalocyanine was used without further purification (Aldrich, 98% purity). The argon gas had a purity of 99.996%.

3. Spectroscopic Analysis of the PcAr$_n$ Clusters

Figure 1 shows two fluorescence excitation spectra measured after doping the helium droplets both with a single phthalocyanine (Pc) molecule as well as with several Ar atoms. For the upper spectrum, Ar was doped prior to Pc, while for the lower spectrum Ar was doped after Pc. In the first case, Pc binds with an Ar cluster of a certain size, while in the latter case a certain number of single Ar atoms are attached to a Pc molecule. Thus, the formation of clusters with Ar attached either to one side of Pc [$(n|0)$ complex] or to both sides [$(n − m|m)$ complex] is favored, respectively.[12] Sharp transitions due to Pc−Ar$_n$ van der Waals clusters differing in the number n of Ar atoms are visible in the spectra shown in Figure 1.

The method for determining the cluster size of Pc−Ar$_n$ relies on the Poisson statistics of the pickup process of molecules or atoms by helium droplets.[9−12] Hence, the intensity $I_n(p)$ of any signal of a specific Pc−Ar$_n$ complex follows the equation:[10,11]

$$I_n(p) = I_n^0 \cdot \frac{\lambda^n}{n!} \cdot e^{-\lambda}, \text{ with } \lambda = \sigma p L / k_B T \qquad (1)$$

where n is the number of Ar atoms in the complex, p is the Ar pressure in the pickup cell, σ is the capture cross-section of Ar by the droplets, L is the length of the droplet beam path through the pickup cell, k_B is the Boltzmann constant, T is the temperature in the pickup cell, and I_n^0 is a constant accounting for the respective transition probability and the sensitivity of the detection system. The intensity $I_n(p)$ of a single PcAr$_n$ transition rises as the n-th power of pressure p with increasing p in the pickup cell reaches a maximum and then falls off again. To determine $I_n(p)$ for all PcAr$_n$ transitions, further excitation spectra covering the same frequency range as those shown in Figure 1 have been recorded for different pressures p in the Ar pickup cell. As an example, the intensities of the four lines at 15073.7, 15069.0, 15055.9, and 15054.1 cm^{-1} are plotted in Figure 2 as functions of the Ar pressure. These data have been fitted with eq 1 for different values of n. On the basis of these fits, the four transitions represent PcAr$_n$ clusters with $n = 1$, 2, 3, and 4, respectively (see solid lines in Figure 2). Such fits have been performed for most of the transitions in the excitation spectrum. The resulting assignment of the transitions to certain PcAr$_n$ clusters is indicated in Figure 1 and summarized in Table 1 together with the transition frequencies of the prominent lines. Additionally, Table 1 lists the frequency shifts $\Delta\tilde{\nu}$ with respect to the 0_0^0 line of bare Pc (15088.9 cm^{-1}) as well as the relative intensity of each line normalized to the most intense signal of the respective cluster size. The Ar pickup pressure p chosen for measuring the spectra in Figure 1 is indicated in Figure 2 by a vertical line. In the following, the bare Pc as well as the different PcAr$_n$ clusters will be discussed in more detail.

3.1. Bare Phthalocyanine (Pc). The signals of bare phthalocyanine (Pc) visible in Figures 1 and 3 a have been assigned previously as summarized in ref 20. The peak at 15088.9 cm^{-1} has been attributed to the electronic origin (0_0^0 line) of Pc in helium droplets since it is the first signal at the low-energy side of the fluorescence excitation spectrum measured at a temperature of 0.38 K.[21] The broad signal at around 15092.7 cm^{-1} has been identified as the phonon wing (PW) of the 0_0^0 line (zero phonon line, ZPL) of Pc in helium droplets.[22,23] Two observations led to this conclusion. First, the frequency shift with respect to the pure molecular signal corresponds to the magnitude of phonon energies expected for helium droplets.[23] Second, the signal saturates at a much higher laser power than the pure molecular transition.[23] The second observation reflects a greatly reduced transition probability of the coupled transition. The weak signal at 15089.5 cm^{-1} has been attributed to the 0_0^0

TABLE 1: Assignment of the Most Prominent Features of the Excitation Spectra Shown in Figure 1

	doping of Ar prior to Pc			doping of Ar after Pc			
	$\tilde{\nu}^a$ (cm^{-1})	$\Delta\tilde{\nu}^b$ (cm^{-1})	rel. int.^{c}	$\tilde{\nu}^a$ (cm^{-1})	$\Delta\tilde{\nu}^b$ (cm^{-1})	rel. int.^{c}	assignment
Pc	15088.9	0	1.00	15088.9	0	1.00	0_0^0
	15089.5	0.6	0.07	15089.5	0.6	0.07	0_0^0 of ^{13}C-Pc
	15092.7	3.8	0.06	15092.7	3.8	0.09	PW
PcAr$_1$	15073.2	−15.7	0.11	15073.2	−15.7	0.24	(1|0)
	15073.7	−15.2	1.00	15073.7	−15.2	1.00	0_0^0 of (1|0)
	15074.3	−14.6	0.07	15074.3	−14.6	0.07	0_0^0 of ^{13}C-(1|0)
	15075.7	−13.2	0.16	15075.7	−13.2	0.31	PW of (1|0)
	15087.6	−1.3	0.04	15087.6	−1.3	0.05	0_0^0
PcAr$_2$				15058.3	−30.6	0.76	0_0^0 of (1|1)
	15068.9	−20.0	1.00	15068.9	−20.0	0.85	0_0^0 of (2|0)
	15069.6	−19.3	0.48	15069.6	−19.3	0.85	0_0^0 of (2|0)
	15069.9	−19.0	0.43	15069.9	−19.0	0.76	(2|0)
	15070.2	−18.7	0.59	15070.2	−18.7	0.79	(2|0)
	15070.4	−18.5	0.63	15070.4	−18.5	0.85	(2|0)
	15070.6	−18.3	0.33	15070.6	−18.3	1.00	0_0^0 of (2|0)
	15071.1	−17.8	0.22	15071.1	−17.8	0.44	(2|0)
PcAr$_3$	15055.9	−33.0	1.00	15055.9	−33.0	0.20	(3|0)
	15057.9	−31.0	0.39				(3|0)
	15060.4	−28.5	0.88				(3|0)
	15061.3	−27.6	0.71				(3|0)
	15062.8	−26.1	0.24	15062.8	−26.1	1.00	0_0^0 of (2|1)
	15067.7	−21.2	0.31				(3|0)
PcAr$_4$	15053.7	−35.2	0.73				(4|0)
	15054.1	−35.8	1.00				(4|0)
	15055.7	−33.2	0.21				(4|0)
	15058.6	−30.3	0.53				(4|0)

^{a} Wavenumber of the observed transition. ^{b} Frequency shift with respect to the 0_0^0 line of Pc at 15088.9 cm^{-1}. ^{c} Relative intensity with respect to the strongest line found for each cluster size.

line of a Pc isotopomer with a ^{13}C atom replacing one of the ^{12}C atoms.[20] The smaller intensity of this line as compared to the intensity of the line at 15088.9 cm^{-1} reflects the abundance of such a Pc isotopomer due to the natural abundance of ^{13}C.[20] In the current experiments, it was found that the weak signal at 15089.5 cm^{-1} exhibits a similar laser power saturation behavior as the 0_0^0 line at 15088.9 cm^{-1}.

In this study, emission spectra have been measured upon excitation at the three transitions of bare Pc in helium droplets discussed above. It will be demonstrated for the example of bare Pc that the emission spectra can be utilized for identifying electronic origins among the multitude of peaks observed in an excitation spectrum of a molecule inside helium droplets. After excitation at the frequencies of the two 0_0^0 transitions (at 15088.9 and 15089.5 cm^{-1}), the origin of the emission spectrum coincides with the respective excitation frequency (see Figure 3b,c). In contrast to that, the origin of the emission spectrum after excitation at the frequency of the PW (at 15092.7 cm^{-1}) appears red-shifted from the excitation frequency (see Figure 3d). The PW at 15092.7 cm^{-1} corresponds to a transition with excess excitation energy of 3.8 cm^{-1} above the ground level of the electronically excited state S$_1$ of Pc in helium droplets. As reported for many organic compounds inside helium droplets, excess excitation energy usually dissipates into the droplet prior to radiation.[18,24,25] Therefore, the emission spectrum after excitation at the frequency of the PW is identical to the emission spectrum observed upon excitation at the ZPL to which the PW is coupled to (see Figure 3b,d).

The origin of the emission spectrum reflects the electronic band origin of the embedded molecule; therefore, the origins of emission and excitation spectrum coincide in the case of excitation at the band origin. Similar as a pump−probe

experiment, the dispersed emission spectra allow for identification of the number of different species contributing to an excitation spectrum. The electronic origin and further excitations are identified for each species.

3.2. PcAr$_1$ Clusters. The signals of the PcAr$_1$ clusters appear in the spectral range between 15073.2 and 15088.9 cm^{-1} as indicated in Figure 1. The following analysis will focus on the strongest peak in this frequency interval at 15073.7 cm^{-1} and on four additional peaks at 15073.2, 15074.3, 15075.7, and 15087.6 cm^{-1} (see Figure 4a). As expected, the signals of PcAr$_1$ are independent of the doping order. As shown in Figure 5a, the intensities $I_n(p)$ of these five transitions follow the same Poisson curve for $n = 1$, proving their assignment to PcAr$_1$. Figure 5b displays the saturation behavior of these five transitions with a plot of intensity vs laser power. The three transitions at 15073.7, 15074.3, and 15087.6 cm^{-1} can be power saturated while the other two transitions at 15073.2 and 15075.7 cm^{-1} show a linear response for the full range of the available laser power.

The excitation spectrum for the PcAr$_n$ clusters is shown in the frequency range from 15091 to 15059 cm^{-1} in Figure 4a to allow for an easy comparison with the emission spectra of the PcAr$_1$ clusters plotted at the same frequency scale in panels b−f. The excitation frequencies of the emission spectra are indicated by vertical arrows. It is readily recognized that for panels c, d, and f, the first line coincides with the excitation frequency while for panel e the emission is shifted to the red as compared to the excitation frequency. The frequencies of the peaks in panel e coincide with those observed in panel c. However, for the emission spectrum shown in panel b, the identification of either a coincidence of the first line with the excitation frequency or a frequency shift to the spectrum shown in panel c is beyond the limit of the spectral resolution.

As reported in ref 24, the triple peak in the emission spectrum upon excitation at 15073.7 cm^{-1} (panel c) represents the emission of the PcAr$_1$ van der Waals complex for three different configurations of the first helium solvation layer. After excitation of the PcAr$_1$ complex, the helium environment may relax with a certain probability into two additional configurations. The transition frequency of the embedded PcAr$_1$ changes when the helium environment changes. Therefore, all transitions of the emission spectrum are split into three lines corresponding to PcAr$_1$ surrounded by the nonrelaxed helium environment and by two different helium configurations. The probability for relaxation of the helium environment depends on the excess excitation energy dissipating into the droplet. Except for the emission spectrum shown in panel f, all other emission spectra show a three-fold split signal. While in panels c and d the spectrum is dominated by the emission without relaxation of the helium environment (first peak within the triple line), the emission after relaxation dominates in panels b and e (second and third peak within the triple line).

In addition to the electronic origin shown in Figure 4a, vibronic transitions of Pc and PcAr$_1$ have been measured. Four sections of the excitation spectrum are plotted in the left column of Figure 6 covering a frequency interval of 20 cm^{-1} each. The top panel shows the spectral range of the Pc and PcAr$_1$ band origins. The lower three panels show three vibronic modes of bare Pc (left peak) and of PcAr$_1$ (right peak). The red shift of the PcAr$_1$ transitions as compared to the transitions of bare Pc is the same for all four vibrational modes, and it amounts to 15.301(2) cm^{-1}. This value has been determined as the mean shift of all together seven lines of PcAr$_1$, three of which are not shown in Figure 6 but are listed in Table 2. Furthermore,

Phthalocyanine−Argon_n Complexes

J. Phys. Chem. A, Vol. 111, No. 31, 2007 **7579**

TABLE 2: Frequencies of the Origin (Bold Numbers) and Several Vibronic Transitions of Pc, PcAr₁, the (1|1) Complex of PcAr₂, Two of the (2|0) Complexes of PcAr₂, and the (2|1) Complex of PcAr₃[a]

Pc	PcAr₁		(1|1)-PcAr₂		(2|0)-PcAr₂				(2|1)-PcAr₃	
$\tilde{\nu}$ (cm⁻¹)	$\tilde{\nu}$ (cm⁻¹)	$\Delta\tilde{\nu}$ (cm⁻¹)	$\tilde{\nu}$ (cm⁻¹)	$\Delta\tilde{\nu}$ (cm⁻¹)	$\tilde{\nu}$ (cm⁻¹)	$\Delta\tilde{\nu}$ (cm⁻¹)	$\tilde{\nu}$ (cm⁻¹)	$\Delta\tilde{\nu}$ (cm⁻¹)	$\tilde{\nu}$ (cm⁻¹)	$\Delta\tilde{\nu}$ (cm⁻¹)
15088.94(1)	**15073.67**(1)	15.27(2)	**15058. 30**(1)	30.64(2)	**15068.93**(1)	20.01(2)	**15070.62**(1)	18.32(2)	**15062.79**(1)	26.15(2)
15217.044(3)	15201.766(6)	15.278(9)								
15314.576(6)	15299.307(8)	15.269(14)								
15653.859(1)	15638.544(2)	15.315(3)	15623.137(4)	30.722(5)			15635.526(6)	18.333(7)	15627.672(3)	26.187(4)
15765.85(5)	15750.635(5)	15.250(10)								
15808.467(2)	15793.171(4)	15.296(6)	15777.801(8)	30.666(10)	15788.50(2)	19.97(2)	15790.17(2)	18.297(22)	15782.360(4)	26.107(6)
15881.963(3)	15866.673(3)	15.290(6)	15851.279(7)	30.684(10)	15861.897(8)	20.07(1)	15863.68(1)	18.283(13)	15855.892(5)	26.071(8)
		Ø = 15.301(2)		Ø = 30.704(4)		Ø = 20.02(3)		Ø = 18. 320(5)		Ø = 26.149(3)

[a] Except for the origins, the transition frequencies have been determined by fitting a Lorentzian to the line shapes. $\Delta\tilde{\nu}$ are the frequency differences of the PcAr_n transitions as compared to the respective Pc transitions.
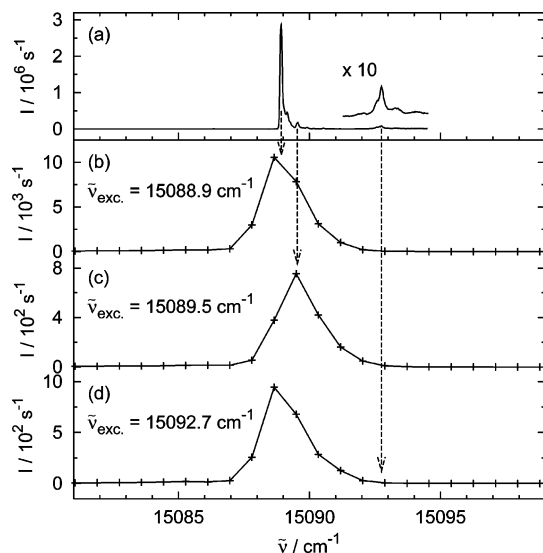

Figure 3. (a) Origin of the fluorescence excitation spectrum of Pc in helium droplets ($\bar{N} \approx 20000$). (b−d) Origins of emission spectra of Pc in helium droplets measured upon excitation at the indicated frequency $\tilde{\nu}_{exc.}$. The dotted arrows mark the excitation frequency. The line width observed in the emission spectra is determined completely by the instrumental resolution.

the line shape and the relative intensity of the Pc and the PcAr₁ signals are identical. Hence, the vibrational modes of Pc are not affected by the Ar atom for this particular PcAr₁ complex.

On the basis of the experimental data reported so far, the five transitions of the PcAr₁ clusters can be assigned as follows. The most intense transition at 15073.7 cm⁻¹ and the signals at 15074.3 and 15087.6 cm⁻¹ represent electronic origins for the following reasons. The emission spectra reveal no energy dissipation prior to radiative decay, which is a clear indication for no excess excitation energy being present. Additionally, all three signals show the typical power saturation of a pure molecular transition. Consequently, the three transitions are assigned to isomeric complexes of the PcAr₁ clusters.

The transitions at 15075.7 and 15073.2 cm⁻¹ cannot be attributed to electronic origins for different reasons. As revealed by the emission spectrum, the signal at 15075.7 cm⁻¹ is linked to the origin at 15073.7 cm⁻¹ and carries excess excitation energy of about 2 cm⁻¹. The low excess excitation energy is typical for a PW of organic molecules in superfluid helium droplets.[23] The saturation behavior reveals a weak transition dipole moment, which is typical for a PW as well. Finally, the intensity distribution in the triple line of the emission spectrum reveals highly efficient relaxation of the helium solvation layer, which is also typical for a PW excitation.[25] Consequently, the signal at 15075.7 cm⁻¹ is attributed to a PW coupled to the ZPL at 15073.7 cm⁻¹. This attribution is not restricted to the
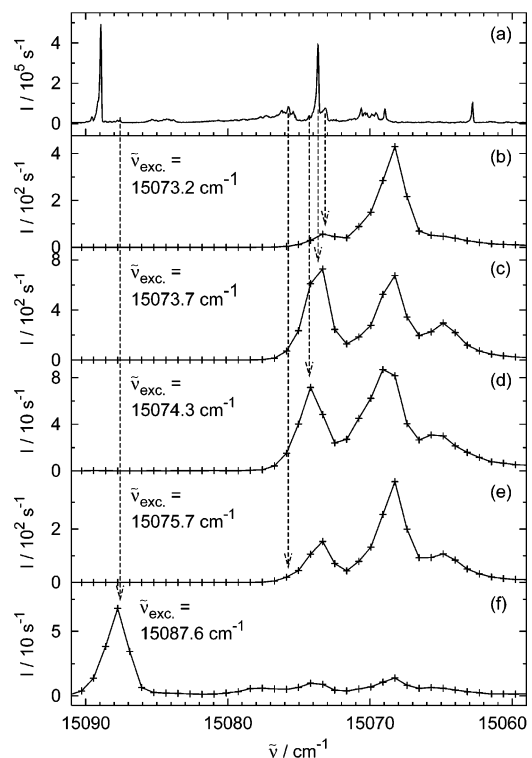

Figure 4. (a) Fluorescence excitation spectrum of PcAr_n in helium droplets ($\bar{N} \approx 20000$) when Ar was picked up after Pc. Note that in the present figure the frequency decreases from left to right. (b−f) Emission spectra of PcAr₁ upon excitation at the frequencies $\tilde{\nu}_{exc.}$ marked with dashed arrows.
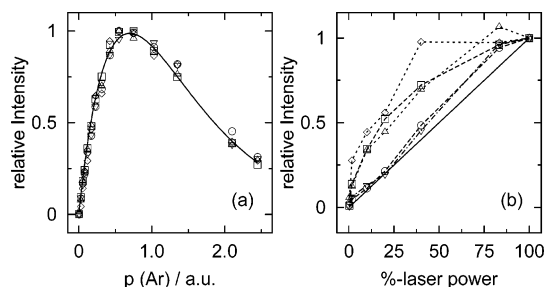

Figure 5. (a) Intensity of the five peaks of PcAr₁ at 15073.7 (□), 15073.2 (⊙), 15074.3 (△), 15075.7 (▽), and 15087.6 cm⁻¹ (◇) as a function of the Ar pressure in the pickup cell. The solid curve represents a fit of the data for the line at 15073.7 cm⁻¹ with eq 1 for $n = 1$. (b) Saturation behavior of the same five transitions with respect to the laser power. The solid line represents a linear intensity dependence.

single peak at 15075.7 cm⁻¹ but holds for the entire structure from 15075 to 15078 cm⁻¹. A possible explanation for the signal at 15073.2 cm⁻¹ is an electronic excitation with both S_1 and S_0 coupled to phonons of the helium environment. This interpreta-
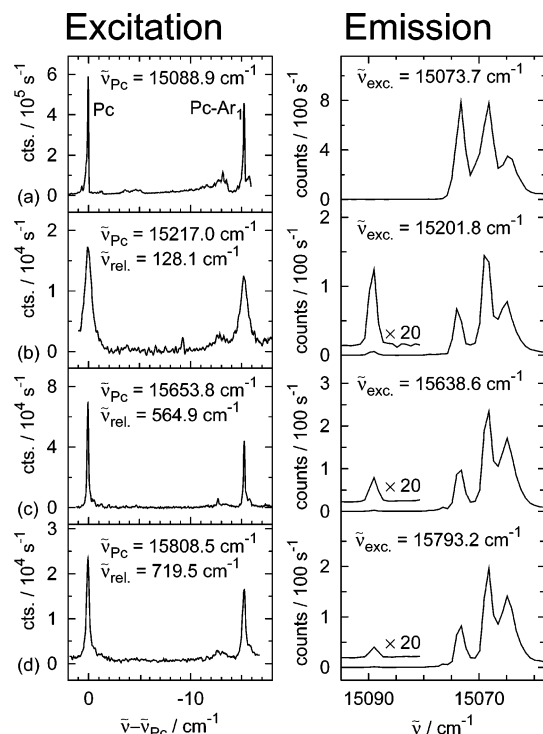
Figure 6. Left column presents four sections of the fluorescence excitation spectrum of Pc and PcAr$_1$. The spectrum in panel a shows the origins of Pc and PcAr$_1$ at 15088.9 and 15073.7 cm^{-1} (see Figure 1). The three spectra in panels b–d represent three vibronic transitions with a relative energy $\tilde{\nu}_{rel.}$ as compared to the respective origin. The right column presents the origin of the emission spectra measured upon excitation at $\tilde{\nu}_{exc.}$, the respective transition of PcAr$_1$ shown to the left. Besides the triply split transition of PcAr$_1$ at 15073, 15068, and 15064 cm^{-1}, the origin of the emission spectrum of Pc in helium droplets at 15089 cm^{-1} can be seen after excitation at a vibronic transition of the PcAr$_1$ complex.
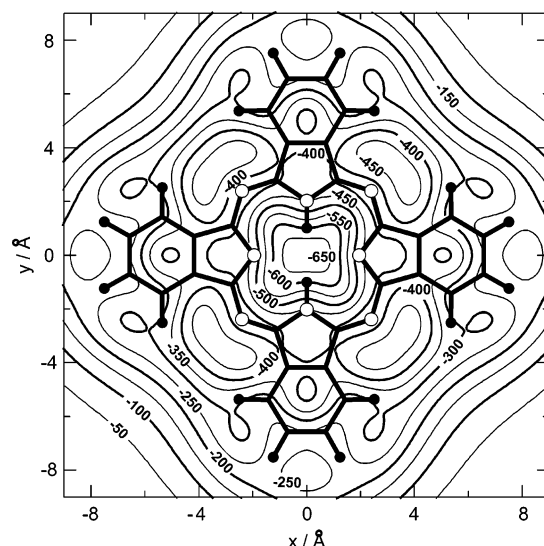

Figure 7. Cut of the three-dimensional Pc−Ar potential energy surface (PES) at a distance of 3.2 Å above the planar phthalocyanine molecule. The open circles represent the nitrogen atoms, and the filled circles represent the hydrogen atoms. The contour lines indicate the potential energy in cm^{-1}.
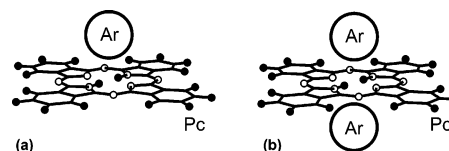

Figure 8. (a) Structure of the PcAr$_1$ complex with the Ar atom in the global minimum position according to the PES shown in Figure 7. The origin at 15073.7 cm^{-1} is assigned to a cluster with this structure. (b) Structure of the (1|1)−PcAr$_2$ complex. The Ar atoms are located in the global minima of the PES on both sides of the Pc molecule. The electronic origin at 15058.3 cm^{-1} is attributed to this complex geometry.

tion is based on the red shift of the excitation frequency with respect to the origin at 15073.7 cm^{-1}, which indicates a hot band possibly starting from a phonon state of the helium environment coupled to S$_0$. Additionally, the intensity pattern within the triple peak in the emission spectrum in Figure 4b reveals dissipation of excess excitation energy, which gives evidence for a final state of the transition being a phonon state coupled to S$_1$.

For the assignment of the transitions to certain structures of the PcAr$_1$ complex, a three-dimensional potential energy surface (PES) for Pc and a single Ar atom has been calculated as a superposition of pairwise Lennard−Jones potentials taking the parameters from refs 2 and 4. In a similar way, a PES for Pc−He has been calculated recently.[26] For the current calculations, the atomic coordinates of Pc were taken from a DFT calculation,[27] which was consistent with experimental data obtained by neutron scattering.[28] The PES exhibits a global minimum of −687 cm^{-1} at a distance of 3.2 Å above the center of the planar phthalocyanine molecule. Additionally, several local minima are found above the periphery of the 18 π conjugated aromatic compound. Figure 7 shows a cut of the PES parallel to the Pc plane at the distance of the global minimum.

The strong intensity of the signal at 15073.7 cm^{-1} and the large red shift with respect to bare Pc suggest that the Ar atom is located at the global minimum position, which is right above the center of mass of Pc (see Figure 7). The identical vibrational structure of this complex and bare Pc supports the assignment of the Ar atom close to the center of mass. In Figure 8a, the PcAr$_1$ complex is shown with the Ar atom in the global

minimum position. The transition at 15074.3 cm^{-1} is located at the higher frequency side of the origin at 15073.7 cm^{-1} with a substantially lower intensity. Similar as to the case of bare Pc (see above), the signals at 15074.3 and at 15073.7 cm^{-1} are attributed to two different isotopomers with one ^{12}C atom replaced by a ^{13}C for the origin at 15074.3 cm^{-1}. Again, the natural abundance of such an isotopomer is reflected by the relative line strength of the two transitions. The third origin at 15087.6 cm^{-1}, which is closer to the origin of bare Pc, is assigned to a complex with Ar located in one of the local minima of the PES of Pc−Ar shown in Figure 7.

3.3. PcAr$_2$ Clusters. Figure 9 shows those sections of the excitation spectra where the prominent transitions of the PcAr$_2$ complexes have been found. The Ar pressure was optimized for an average pickup of three argon atoms leading to a maximum signal for the PcAr$_3$ complexes. The PcAr$_2$ cluster is the smallest one sensitive to the doping order. The most remarkable effect on the doping sequence was observed for the line at 15058.3 cm^{-1}, which appeared with high intensity for doping Ar after Pc (dashed line) and is almost absent for the reversed doping order (solid line). In contrast to that, the PcAr$_2$ signals in the frequency range from 15067.9 to 15072.1 cm^{-1} show a higher intensity for doping Ar prior to Pc. Therefore, the signal at 15058.3 cm^{-1} is attributed to a (1|1) complex while the other transitions in the frequency ranging from 15067.9 to 15072.1 cm^{-1} are assigned to (2|0) complexes of the PcAr$_2$ clusters.

Emission spectra were measured upon excitation at the transition of the (1|1) complex (at 15058.3 cm^{-1}) and at three

Phthalocyanine−Argon$_n$ Complexes
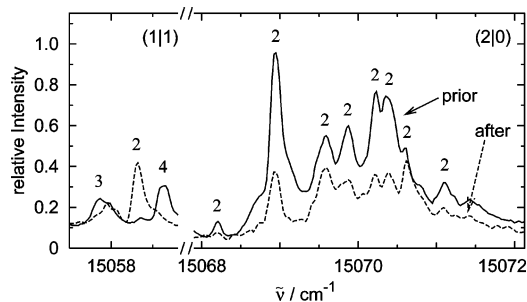
J. Phys. Chem. A, Vol. 111, No. 31, 2007 **7581**

Figure 9. Two parts of the fluorescence excitation spectrum of PcAr$_n$ complexes from 15057.5 to 15058.8 cm^{-1} and from 15067.9 to 15072.1 cm^{-1}. The numbers 2, 3, and 4 indicate the assignment of the peaks to PcAr$_2$, PcAr$_3$, and PcAr$_4$, respectively. The excitation spectra measured by doping Ar prior to Pc or after Pc are shown as solid and dashed lines, respectively. The PcAr$_2$ line at 15058.3 cm^{-1} is assigned to the (1|1) complex, while the PcAr$_2$ lines between 15067.9 and 15072.1 cm^{-1} are attributed to (2|0) complexes.
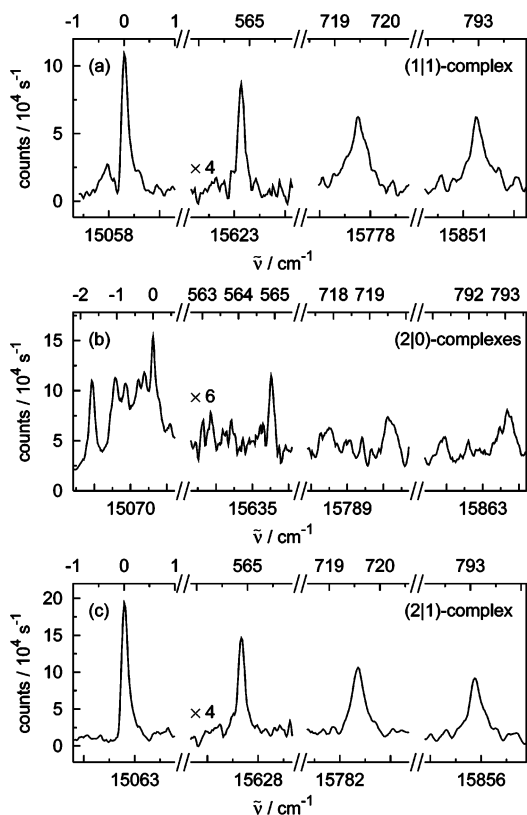

Figure 10. (a) Fluorescence excitation spectra of the band origin as well as three vibronic transitions of (a) the (1|1) complex of PcAr$_2$, (b) some of the (2|0) complexes of PcAr$_2$, and (c) the (2|1) complex of PcAr$_3$. The scale on top of the spectra gives the frequency relative to the respective origin at (a) 15058.3, (b) 15070.6, and (c) 15062.8 cm^{-1}.

transitions of the (2|0) complexes (at 15068.9, 15069.6, and 15070.6 cm^{-1}). In all four cases, the origin of the emission spectrum coincides with the respective excitation frequency. Consequently, these four lines represent electronic origins of different isomers. This demonstrates that the addition of two Ar atoms to one side of Pc leads already to a large number of different structures that are realized in the helium droplets.

Vibronic transitions have been measured for the (1|1) complex and for some of the (2|0) complexes (see Figure 10a,b). The top axes give a relative scale related to the origins at 15058.3 and 15070.6 cm^{-1} for panels a and b, respectively. The vibrational frequencies, the relative intensities, and the line widths of the vibronic transitions for the two PcAr$_2$ complexes are identical to those found for bare Pc in helium droplets.
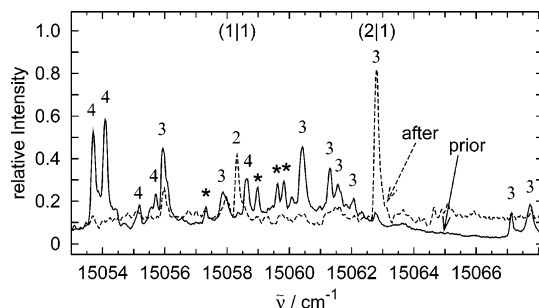

Figure 11. Fluorescence excitation spectra of PcAr$_n$ clusters optimized for $n = 3$. The solid and the dashed line represent the spectra measured for doping of the Ar atoms prior to or after the Pc molecule, respectively. The numbers 3 and 4 indicate the assignment of the lines to PcAr$_3$ and PcAr$_4$, respectively. For the peaks marked with a star (*), it could not be determined if they belong to PcAr$_3$ or PcAr$_4$.

Therefore, it is likely that for these two complexes the Ar atoms are located close to the center of mass of the Pc molecule. In case of the (1|1) complex, we propose that the two Ar atoms are located at both sides of the planar Pc molecule right above the center of the aromatic ring (see Figure 8b), which is in agreement with the global minimum of the PES of Pc−Ar (see Figure 7). Further evidence for this assignment lies in the red shift of 30.704(4) cm^{-1} of the excitation spectrum as compared to bare Pc, which is twice as large as for the spectrum of PcAr$_1$ with the Ar atom at the global minimum position. For the (2|0) complexes, some structural information can be extracted from the vibronic transitions (see Figure 10b). Strong vibronic transitions can only be observed for the complexes with an origin at 15068.9 and at 15070.6 cm^{-1}. Therefore, the two argon atoms have small influence on the Pc vibrations and might both be located in the global minimum right above the center of mass, forming a dimer. In case of the (2|0) complex with the origin at 15070.6 cm^{-1}, the two Ar atoms are expected to form a dimer with its symmetry axis orthogonal to the Pc plane located in the global minimum right above the center of mass of Pc. Further evidence for this assignment is given by the emission spectra discussed in section 4.

3.4. PcAr$_3$ and PcAr$_4$ Clusters. Figure 11 shows the fluorescence excitation spectrum of the PcAr$_n$ complexes in the frequency range from 15053 to 15068.15 cm^{-1}. The prominent signals of the PcAr$_3$ and PcAr$_4$ clusters have been found in this region. For both spectra, the Ar pickup pressure was optimized for an average doping with three Ar atoms. Some peaks [marked with an asterisk (*)] cannot be classified as PcAr$_3$ or PcAr$_4$, because their intensity dependence on the Ar pickup pressure $I_n(p)$ lies in between the curves found for $n = 3$ and $n = 4$. This observation can be explained by spectral overlap of signals of PcAr$_3$ with those of PcAr$_4$.

For the dashed excitation spectrum (doping of Ar after Pc), only two sharp lines were identified as PcAr$_3$ clusters (at 15055.9 and 15062.8 cm^{-1}). For the reverse doping sequence (solid line), the intensity of the line at 15055.9 cm^{-1} is approximately doubled while the line at 15062.8 cm^{-1} is hardly recognized. Thus, the line at 15062.8 cm^{-1} is assigned as a (2|1) complex. The peak at 15055.9 cm^{-1} as well as all of the other PcAr$_3$ transitions that are only visible when doping with Ar prior to Pc are assigned as (3|0) complexes (see also Table 1).

An emission spectrum was measured upon excitation at 15062.8 cm^{-1}. The origin of this spectrum coincided with the excitation frequency. Consequently, the transition at 15062.8 cm^{-1} represents the electronic origin (0_0^0 line) of the excitation spectrum of a (2|1) complex. Moreover, vibronic transitions of the (2|1) complex have been measured and are shown in Figure

10c. The vibrational frequencies and the line shapes were identical to those observed for bare Pc in helium droplets (see Figure 6). Therefore, the three Ar atoms are expected to be located close to the center of mass of the Pc molecule.

The signals of $PcAr_4$ clusters are visible for doping Ar prior to Pc but are entirely absent for the reverse doping order (see Figure 11). Thus, within this spectral range, all $PcAr_4$ clusters are identified as (4|0) complexes.

3.5. Discussion of the Structure of the $PcAr_n$ Clusters. The cluster size as well as the structure of some particular $PcAr_n$ complexes in helium droplets could be determined from excitation and emission spectra. All $PcAr_n$ clusters with more than one Ar atom showed a significant larger number of isomeric complexes for doping with Ar prior to Pc. Consequently, the variety of isomeric complexes found for the (n|0) configuration is larger than for the (n − m|m) configuration. It can be assumed that the corrugation of the potential energy surface shown in Figure 7 for a single Ar atom decreases for a cluster of Ar atoms. Consequently, the approach of a single Pc molecule to an Ar_n cluster at random orientation does not lead necessarily to a global minimum configuration as is the case for the consecutive pickup of single Ar atoms after doping with Pc. Thus, the number of isomeric complexes formed in helium droplets appears to be determined by the random orientation of both the Pc molecule and the Ar cluster rather than by a limited number of global and local energy minima.

Van der Waals clusters of $PcAr_n$ have also been investigated in a supersonic jet expansion.[7] Except for a spectrally broad signal due to hot bands, two sharp transitions appeared when seeding the jet expansion in Ar. They were shifted to the red as compared to the bare Pc by about 15 ± 2 and 30 cm^{-1}, respectively, and have been identified as a $PcAr_1$ and a $PcAr_2$ cluster. In helium droplets, a $PcAr_1$ complex and a (1|1)−$PcAr_2$ complex with similar red shifts have been found. The (1|1)−$PcAr_2$ signal, however, was absent for doping Ar prior to Pc. Obviously, creating clusters in helium droplets by doping Ar after Pc is similar to the process of condensation of single Ar atoms to an isolated Pc molecule while for the reversed doping order the Pc molecule is attached to a solid Ar cluster. Besides the doping order, the low temperature provided by the superfluid helium environment has an influence on the spectra. The most significant one is that in helium droplets the contributions of hot bands are negligible. Therefore, the spectrum is simplified allowing for detection of metastable configurations.

4. Dynamic Processes

The emission spectra of the $PcAr_n$ clusters also reveal information on dynamic processes. For example, the emission spectra of the most intense $PcAr_1$ complex show an additional line at 15089 cm^{-1} for excitation upon vibronic transitions in contrast to excitation at the electronic origin at 15073.7 cm^{-1} (see right column of Figure 6a−d). The transition frequency of 15089 cm^{-1} represents the origin of bare Pc in helium droplets. Because the three vibronic excitations of $PcAr_1$ used for measuring the emission spectra do not overlap with any transition of bare Pc, the emission at 15089 cm^{-1} reveals vibrational predissociation of the excited $PcAr_1$ complex. An excess energy of 113 cm^{-1} is sufficient for dissociation of the van der Waals bond. This value is determined as the difference between the lowest excitation frequency for which predissociation has been observed ($\tilde{\nu}_{exc.}^{diss.}$ = 15202 cm^{-1}) and the frequency of the Pc line ($\tilde{\nu}_{Pc}$ = 15089 cm^{-1}). Consequently, the binding energy D_0 of the $PcAr_1$ complex in a helium droplet can be estimated to be $D_0 \leq \tilde{\nu}_{exc.}^{diss.} - \tilde{\nu}_{Pc} = 113$ cm^{-1}. The

transition frequency of 15089 cm^{-1} proves that the Pc fragment remains inside the helium droplet while the Ar atom is at a distance with negligible interaction to the Pc fragment. It cannot be determined directly with our experiments whether the Ar atom stays inside the droplet or leaves the droplet after the dissociation of the $PcAr_1$ complex. However, the binding energy of one Ar atom to a helium droplet has been estimated to be 220 cm^{-1},[9] which is larger than the available excess energy of 113 cm^{-1}. Therefore, it can be assumed that the Ar atom stays inside the helium droplet after dissociation of the $PcAr_1$. The helium droplets used for the current experiments ($\bar{N} = 20000$) have initially a diameter of about 120 Å ($R = 2.22 \sqrt[3]{N}$[15]). If the evaporative loss due to the pickup of a Pc molecule (3000 atoms[29]) and an Ar atom (244 atoms[9]) is taken into account, the diameter of the droplet will still be 114 Å. It was calculated that the potential energy drops to about 1% of the potential energy at the global minimum (see Figure 7) if the Ar atom is at a distance of about 10 Å over the center of the Pc molecule. Hence, the size of the droplet is sufficiently large to fit both the Ar atom and the Pc molecule without noticeable interaction. In the gas phase, an excess energy of at least 661 cm^{-1} is required for vibrational predissociation.[7] As can be seen in Figure 7, the dissociation threshold in the gas-phase experiment is consistent with the binding energy of the van der Waals complex in the global minimum configuration. Hence, the helium environment drastically reduces the dissociation energy of this van der Waals complex. The binding energy of $PcAr_1$ in gas phase represents the energy that is released if an isolated Ar atom binds to an isolated Pc molecule. In helium droplets, however, the binding energy of $PcAr_1$ equals the energy that is released if a solvated Ar atom and a solvated Pc molecule form a solvated $PcAr_1$ complex. For this process, some of the solvating He atoms that are bound to the Ar and the Pc have to be removed. The energy required for breaking these bonds reduces the binding energy of $PcAr_1$ in helium droplets as compared to the gas-phase value.

Interestingly, no vibrational predissociation was observed for the $PcAr_2$ complexes. However, some of the emission spectra upon excitation at vibronic transitions revealed a dynamic process of a different type, namely, the interconversion between different complex configurations. Isomerization of molecular complexes inside helium droplets has been observed previously for the complexes of HCN and HF using infrared−infrared double resonance spectroscopy.[30] In Figure 12, four emission spectra of the (1|1) complex and of one of the (2|0) complexes are shown as solid and dashed lines, respectively. Panel a presents the spectra upon excitation at the respective origin at 15058.3 and at 15070.6 cm^{-1}, whereas panels b−d show emission spectra of both complexes upon excitation at vibronic transitions. In Figure 10a,b, the transitions are shown that have been chosen for measuring the four emission spectra in Figure 12. Upon excitation at the respective origin of the two complexes (see Figure 12a), the emission spectra of both clusters are shifted with respect to each other by 12.3 cm^{-1} corresponding to the difference of the excitation frequencies. Both spectra show the same vibrational frequencies as observed for Pc.[18] Upon excitation at three vibronic transitions (see Figure 12b−d), the emission spectra of the (1|1) complex do not change as compared to the spectrum upon excitation at the origin (see Figure 12a). The emission spectra of the (2|0) complex upon vibronic excitation, however, consist of two components in contrast to the emission spectrum upon excitation at the origin. The first component coincides with the spectrum observed upon excitation at the origin and the second one coincides with the
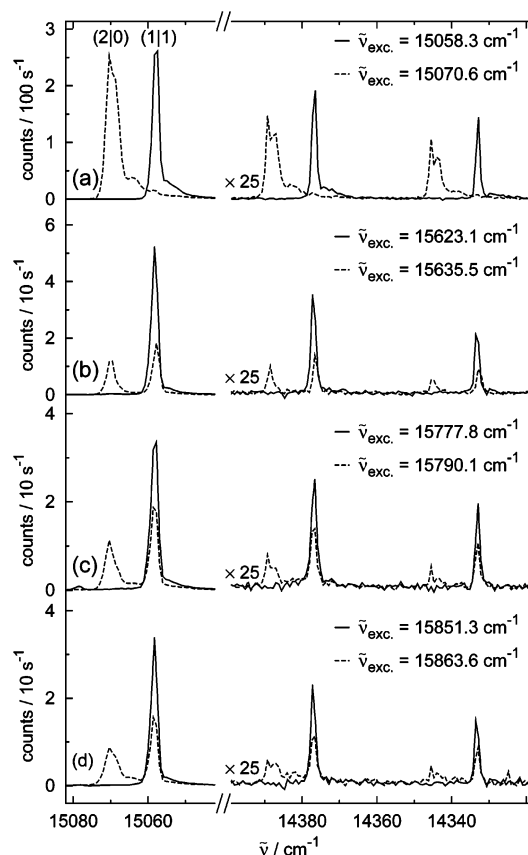
Phthalocyanine−Argon$_n$ Complexes

J. Phys. Chem. A, Vol. 111, No. 31, 2007 **7583**

Figure 12. Emission spectra of the (1|1) PcAr$_2$ complex (solid lines) and of the (2|0) PcAr$_2$ complex (dotted lines) in the frequency ranges from 15082 to 15042 cm^{-1} and from 14399 to 14319 cm^{-1} presenting the origin as well as two vibronic transitions. The excitation frequencies $\tilde{\nu}_{exc.}$ are given. Part a shows the emission spectra upon excitation at the origins, and parts b−d present the spectra after excitation at three vibronic transitions.
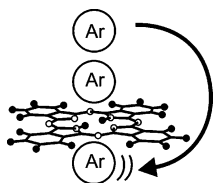

Figure 13. Sketch of the mechanism proposed for the interconversion process leading from the (2|0) complex to the (1|1) complex.

emission spectrum of the (1|1) complex. The intensity ratio of the two components is almost independent of the vibronic excitation energy. It is concluded that, upon vibronic excitation, one of the two Ar atoms migrates to the opposite side of Pc leading to an isomerization to the (1|1) complex with the origin at 15058.3 cm^{-1}. This process is independent of the amount of excess excitation energy. Such an interconversion was found only for the (2|0) complex with the origin at 15070.6 cm^{-1}. To explain the isomerization process, a structure is proposed for this particular (2|0) complex where an Ar dimer is aligned vertically to the Pc plane right above the center of mass of Pc (see Figure 13). For the conversion into a (1|1) complex, the weakly bound outer Ar atom flips to the opposite side of Pc into the global minimum position. Taking into account the diameter of Pc in the order of 1 nm (see Figure 7) and the fluorescence life time in the order of 10 ns, the speed necessary for changing from one side to the opposite side of the Pc molecule within the excited-state life time is about 0.1 m/s. This is significantly lower than the Landau velocity of 58 m/s;[31−33] thus, the migration is expected to proceed without friction

through the superfluid helium. For the proposed complex configuration, the migrating Ar atom is outside of the nonsuperfluid first solvation layer,[26] which is favorable for the migration. The small red shift of 18.32 cm^{-1} found for the (2|0) complex that undergoes isomerization is only about 3 cm^{-1} larger than that of the most prominent PcAr$_1$ signal. This observation supports the structural assignment of the (2|0) complex since it speaks for a location of the second Ar atom at a larger distance from the Pc molecule than the first Ar atom. However, tunneling through the center of Pc cannot be ruled out as the configuration conversion path. Already minor motions caused by the vibrational modes of Pc may influence, and thus increase, the tunneling probability significantly.

5. Conclusion

The fluorescence excitation spectra as well as the emission spectra of phthalocyanine−argon complexes with up to four Ar atoms have been recorded (PcAr$_n$, $n = 1−4$). These complexes have been formed inside cold (0.38 K[16]), superfluid helium droplets with a mean size of about 20000 atoms per droplet. Besides the most prominent clusters of PcAr$_1$ and PcAr$_2$ also visible in a supersonic jet expansion,[7] additional sharp lines have been observed. Poisson statistics and alternating pickup sequence were used to identify the cluster size and the binding side of the Ar atom, either single-sided (n|0) or double-sided ($n − m$|m), for most of the signals. With the help of emission spectra, it was possible to identify the electronic origins of isomeric complexes.

Doping with Ar after Pc leads to the same complex configurations as known in the gas phase.[7] For the reversed doping order, the configuration distribution is changed dramatically. The complexes observed in the gas phase are much less abundant, and different complex configurations are favored. This might be expected for any cluster of this type consisting of a single planar molecular chromophore and a number of rare gas atoms. As shown already for water clusters[34] or HCN clusters,[35] the helium environment stabilizes complex configurations that are not known from the gas phase. In the case of herterocluster, the doping order has great influence on the complex configuration. This needs to be considered when using helium droplets as a host system for the investigation of bimolecular or larger complexes.

Besides detailed structural information, the emission spectra revealed surprising dynamic processes of the van der Waals clusters such as vibrational predissociation of an PcAr$_1$ cluster and conformational changes among the PcAr$_2$ clusters. Predissociation was observed for the most prominent PcAr$_1$ cluster at an excess excitation energy of less that 20% of the theoretical and experimental value obtained for the respective gas-phase system.[7] Conversion of a (2|0) cluster into a (1|1) cluster was found after vibronic excitation. It could be demonstrated that excitation and emission spectroscopy enable the study of a variety of properties of van der Waals complexes in helium droplets such as cluster size, shape of the clusters, identification of isomers, vibrational predissociation, and conformational relaxation.

References and Notes

(1) Amirav, A.; Even, U.; Jortner, J. *J. Chem. Phys.* **1981**, *75*, 2489.

(2) Ondrechen, M. J.; Berkovitch-Yellin, Z.; Jortner, J. *J. Am. Chem. Soc.* **1981**, *103*, 6586.

(3) Even, U.; Amirav, A.; Leutwyler, S.; Ondrechen, M. J.; Berkovitch-Yellin, Z.; Jortner, J. *Faraday Discuss. Chem. Soc.* **1982**, *73*, 153.

(4) Even, U.; Jortner, J.; Berkovitch-Yellin, Z. *Can. J. Chem.* **1985**, *63*, 2073.

(5) Troxler, T.; Knochenmuss, R.; Leutwyler, S. *Chem. Phys. Lett.* **1989**, *159*, 554.

(6) Ben-Horin, N.; Even, U.; Jortner, J. *J. Chem. Phys.* **1992**, *97*, 5296.

(7) Cho, S. H.; Yoon, M.; Kim, S. K. *Chem. Phys. Lett.* **2000**, *326*, 65.

(8) Tang, J.; Xu, Y.; McKellar, A. R. W.; Jäger, W. *Science* **2002**, *297*, 2030.

(9) Lewerenz, M.; Schilling, B.; Toennies, J. P. *J. Chem. Phys.* **1995**, *102*, 8191.

(10) Hartmann, M.; Miller, R. E.; Toennies, J. P.; Vilesov, A. F. *Science* **1996**, *272*, 1631.

(11) Hartmann, M.; Lindinger, A.; Toennies, J. P.; Vilesov, A. F. *Chem. Phys.* **1998**, *239*, 139.

(12) Pörtner, N.; Vilesov, A. F.; Havenith, M. *Chem. Phys. Lett.* **2001**, *343*, 281.

(13) Grebenev, S.; Sartakov, B.; Toennies, J. P.; Vilesov, A. *Phys. Rev. Lett.* **2002**, *89*, 225301.

(14) Stienkemeier, F.; Lehmann, K. K. *J. Phys. B* **2006**, *39*, R127.

(15) Brink, D.; Stringari, S. *Z. Phys. D* **1990**, *15*, 257.

(16) Hartmann, M.; Miller, R. E.; Toennies, J. P.; Vilesov, A. *Phys. Rev. Lett.* **1995**, *75*, 1566.

(17) Toennies, J. P.; Vilesov, A. F. *Annu. Rev. Phys. Chem.* **1998**, *49*, 1.

(18) Lehnig, R.; Slenczka, A. *J. Chem. Phys.* **2003**, *118*, 8256.

(19) Lewerenz, M.; Schilling, B.; Toennies, J. P. *Chem. Phys. Lett.* **1993**, *206*, 381.

(20) Lehnig, R.; Slipchenko, M.; Kuma, S.; Momose, T.; Sartakov, B.; Vilesov, A. *J. Chem. Phys.* **2004**, *121*, 9396.

(21) Hartmann, M. *Hochauflösende Spektroskopie von Molekülen in* ^{4}*Helium- und* ^{3}*Helium-Clustern*; Dissertation, ISSN: 0436-1199; Max-Planck-Institut für Strömungsforschung: Göttingen, 1997.

(22) Slenczka, A.; Dick, B.; Hartmann, M.; Toennies, J. *J. Chem. Phys.* **2001**, *115*, 10199.

(23) Hartmann, M.; Lindinger, A.; Toennies, J.; Vilesov, A. *Phys. Chem. Chem. Phys.* **2002**, *4*, 4839.

(24) Lehnig, R.; Slenczka, A. *Chem. Phys. Chem.* **2004**, *5*, 1014.

(25) Lehnig, R.; Slenczka, A. *J. Chem. Phys.* **2005**, *122*, 244317.

(26) Whitley, H. D.; Huang, P.; Kwon, Y.; Whaley, K. B. *J. Chem. Phys.* **2005**, *123*, 054307.

(27) Gong, X.; Xiao, H.; Tian, H. *Int. J. Quantum Chem.* **2002**, *86*, 531.

(28) Hoskins, B.; Mason, S.; White, J. *J. Chem. Soc. D: Chem. Commun.* **1969**, *10*, 554.

(29) Dick, B.; Slenczka, A. *J. Chem. Phys.* **2001**, *115*, 10206.

(30) Douberly, G. E.; Merritt, J. M.; Miller, R. E. *Phys. Chem. Chem. Phys.* **2005**, *7*, 463.

(31) Landau, L. *Phys. Rev.* **1941**, *60*, 356−358.

(32) Allum, D. R.; McClintock, P. V. E.; Phillips, A.; Bowley, R. *Phil. Trans. R. Soc. London A* **1977**, *284*, 179.

(33) Donnelly, R. J.; Barenghi, C. F. *J. Phys. Chem. Ref. Data* **1998**, *27*, 1217.

(34) Nauta, K.; Miller, R. E. *Science* **2000**, *287*, 293.

(35) Nauta, K.; Miller, R. E. *Science* **1999**, *283*, 1895.